Available online at www.elixirpublishers.com (Elixir International Journal)

Corrosion and Dye

Elixir Corrosion & Dye 91 (2016) 38510-38518

ISSN: 2229-712X

Psidium Guajava Leaf as Green Corrosion Inhibitor for Carbon Steel in Sulfamic Acid Solutions

A. S. Fouda[1*], S. A. Abd El-Maksoud[2], M. Sh. Zoromba[2] and A. R. Ibrahim[1]

[1]Department of Chemistry, Faculty of Science, Mansoura University, Mansoura-35516, Egypt.

[2]Department of Chemistry, Faculty of Science, Port Said and King AbdulazizUniversity, Port Said, Egypt and KSA.

ARTICLE INFO

Article history:

Received: 31 December 2015;

Received in revised form:

18 February 2016;

Accepted: 23 February 2016;

Keywords

Corrosion inhibitors,

Sulfamic acid,

C-steel surface,

Surface morphology.

ABSTRACT

The effect of Psidium guajava leaf as corrosion inhibitors in 10 % sulfamic acid solution was conducted using different techniques at temperatures 298 K.The effect of temperature was studied and activation and adsorption thermodynamic parameters were computed and discussed. The surface morphology was analyzed using scanning electron microscope (SEM). Potentiodynamic polarization studies showed that Psidium guajava leaf acts as mixed type inhibitor for corrosion of C-steel in 10% NH_2SO_3H solution. The addition of Psidium guajava leaf led to increase in the charge transfer resistance (R_{ct}) and decrease in capacitance of the double layer (C_{dl}). The inhibition mechanism involve physisorption. The adsorption of this extract on C-steel surface obeys isotherm. All studied techniques gave similar results. Surface of C-steel was analyzed using scanning electron microscopy (SEM) technique.

© 2016 Elixir all rights reserved.

Introduction

C-steel is the extended metal used in industrial purpose, Army equipment, building and more in manufacturing of installations for petroleum, fertilizers and other industry. So the protection of C-steel in aqueous solutions is universal request, Economical, environmental, and aesthetical important[1]. The use of inhibitor is more effective way to reduce the corrosion of C-steel. The organic compoundsare widely used as corrosion inhibitors as it contains heteroatom such as O, N, P, S, and heavy metals. But the organic compounds are hazards and unfriendly environment inhibitors[2].In spite of the broad spectrum of organic compounds available as corrosion inhibitors, there is increasing concern about the toxicity of most corrosion inhibitors because they are toxic to living organism and may also poison the earth [3]. These have prompted searches for green corrosion inhibitors. According to Eddy et al. [4], green corrosion inhibitors are biodegradable and do not contain heavy metals or other toxic compounds. The successful use of naturally occurring substances to inhibit the corrosion of metals in acidic and alkaline environment has been reported by some research groups[5-11].

The present research will discuss the "Psidium guajava leaf" as green corrosion inhibitor which as renewable source, friendly environmental acceptance, biodegradable, safer and cheaper than other green corrosion inhibitors for protecting C-steel in 10% NH_2SO_3H medium. Sulfamic acid 10% NH_2SO_3H is selected for present study, due to its wide industrial applications such as acid pickling, acid cleaning, water cooling and circulation or acid heat exchanger[12].

Plant extract preparation

Psidium guajava leafwere dried in the shade at room temperature and grind using electrical mill into fine powder, then take one g of powder in 500 ml measuring flask and dissolved in bidistilled water and leave the flask on the hot plate, after that the solution leave too cool at room temperature then filtrate. Take 10 ml filtrate + 5ml ethanol in condensate-collecting flask of rotary evaporatorto determined concentration of dissolved substance in plant extract solution. The remained weight of dry substance in collection flask after evaporate the solvent equal the equivalent weight dissolved 10 ml filtrate. By this relation we can prepare stock plant extract solution with desired concentration [13].

Figure 1. Psidium guajava leaf

Experimental

Composition of material samples

Solutions

The corrosive media is sulfamic acid (10% NH_2SO_3H) were prepared from solid sulfamic acid purity 99.8% by dilution by bidistilled water.

Tele:

E-mail address: asfouda@hotmail.com

© 2016 Elixir all rights reserved

Table 1. Chemical composition (weight %) of C-steel

Elements	C	Cr	Ni	Si	Mn	P	S	Fe
Composition (weight %)	0.14	0.1	0.01	0.024	0.5	0.05	0.05	Rest

Gravimetric Technique

Weight loss measurements of six similar prepared C-steel coupons with dimension (2.0x2.0x0.2)cm. which abraded with various grade emery papers up to 2000, then washed with bidistilled water and acetone, then weighed. The coupons were suspended in 100 ml of 10% NH_2SO_3H with and without addition of different concentrations of Psidium guajava leaf extract. Through period time 30 min. takeout coupons, washed, dried and re-weighted accurately through 3hr. at various temperatures from 298 to 328 K [14, 15].

The mean weight losses were obtained. The surface coverage θ and inhibition efficiency IE%. Can be obtained from equation (1):

$IE\% = \theta \times 100 = [1-(W / W^o)] \times 100$ (1)

Where, W and W^o are the mean weight losses with and without addition of Psidium guajava respectively. Corrosion rate was calculated using equation (2):

Corrosion Rate $k = W/ A\,xt$ (2)

Where,

W is weight loss at certain time (t) in min and (A) area in cm^2. [16]

Electrochemical Techniques

Electrochemical experiments were carried out using cell consists of three electrodes (a) Working electrode is $1cm^2$ C-steel welded with Cu-wire for electrical connection and mounted into glass tube of appropriate diameter and use epoxy resin to make the contact area of the electrode to be 1 cm^2. This electrode is abradedas before. [24](b) Reference electrode is saturated calomel electrode SCE. Used directly in contact with working solution, while all potential value were recordedvs. SCE. Lugging-Haber capillary tube was also include in the design, Lugging capillary tip is made very close to the surface of the working electrode minimize IR drop. [17](c) Platinum foil ($1cm^2$) as auxiliary electrode. All electrochemical measurements were performed in solution 10% NH_2SO_3H in presence and absence various concentrations of the extract at 298 K under un-stirred and aerated conditions. The measurements were performed using Gamry instrument Potentiostat / Galvanostat, ZRA(PCI4-G750), this include Gamry applications include DC105 software for DC corrosion, EIS300 software for electrochemical impedance spectroscopy, and EFM140 for electrochemical frequency modulation measurements along with computer for collecting data and analysis it by use Echem analyst V.6.03 used for plotting, graphing, and fitting the result data.

Open circuit potential (OCP)

The first step in electrochemical experiment. Working electrode was measure as function oftime during 1hr. this time necessary to reach steady stateand obtain (OCP) value.

Non-destructive method

(a) EIS measurements were carried outin frequency range from 0.3 Hz to 100 KHz with amplitude of 5 mV peak to peak using Ac signals at open circle potential. The experimental impedance was analyzed and interpreted based on the equivalent circuit. The main parameter deduced from EIS analysis are R_{ct} charge transfer resistance, capacitance of double layer,C_{dl}. Inhibition efficiency (IE %)and surface coverage (Θ) were defined by this equation (3).

$IE\% = \theta \times 100 = [1-(R^\circ_{ct} / R_{ct})] \times 100$ (3)

Where

R°_{ct}, R_{ct} are the charge transfer resistance in the absence and presence of extract, respectively[18].

(b) EFM measurements were carried out using two frequency 2 and 5 Hz. The base frequency was 0.1 Hz, so the wave form repeat after 1 sec. the higher frequency must me at least two time the lower one. The higher frequency must also be sufficiently slow that the charging of double layer dose not contribute to the current response. Often 10 Hz reasonable limit. The intermodulation spectra contain current responses assigned for harmonically and intermodulation current peak. The large peaks were used to calculate the corrosion current density ($i_{corr.}$), the Tafel slopes (β_c and β_a) and the causality factors CF-2&CF-3.[19, 20]

Destructive method

This method include DC potentiodynamic polarization technique which was used todetermine corrosion current density under steady state conditions by applying potential from-600 to +600 mV to obtain Tafel polarization curve and the result current is plotted as logarithm scale vs potential related to SCE, Extrapolating of two Tafel regions give ($i_{corr.}$) and ($E_{corr.}$) corrosion potential. By ($i_{corr.}$) we able to calculate rate of corrosion (R) = 0.13($i_{corr.}$) (Equivalent weight)/ D where, D is density in g/cm^3[21].

Equation (4) was used to determine IE% and Θ: $IE\% = \theta \times 100 = [1-(i_{corr} / i^o_{corr})] \times 100$ (4)

Surface examination

Preparation of C-steel surface by keeping the coupons for 24 hrsin 10% NH_2SO_3H in the presence and absence the extract, after abraded using different emery papers up to 2000 grade size then the coupons were washed gently with bidistilled water, carefully dried and mounted into desiccator without any further treatment. The corroded C-steel were examined using an X-ray diffractometer Philips (pw-1390)with Cu-tube (Cu Ka1, I = 1.5405 A°), scanning electron microscope (SEM, JSM-T20, Japan).

Results and Discussion

Gravimetric Technique

Weight loss of C-steel was determined at various time interval in the absence and presence of different concentrations on extract. Figure 2 shows the weight loss-time curves for C-steel in 10%NH_2SO_3H in the absence and presence of various concentrations of extract at 298 °K. This figure shows that the curves in the presence of the extract falls significantly below that of free acid.

The calculated values of corrosion rate (k) and surface coverage(θ) and inhibition efficiency(IE %)obtained from weight loss measurement for various concentration of inhibitor in 10%NH_2SO_3H at 298-328°K are listed in Table. It is evident from this Table 2 and Figure 3 that the corrosion rate increased by increasing the temperature and the %IE increased by increasing the concentration of the extract and on the other hand, decreased by increasing the temperature.

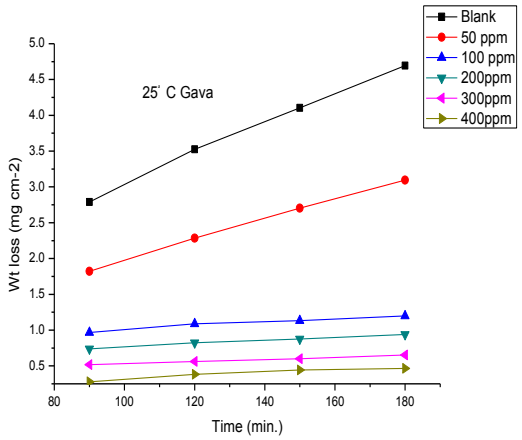

Figure 2. Weight loss-time curves for the corrosion of C-steel in 10%NH_2SO_3H in the absence and presence of various concentrations of extract at 298K.

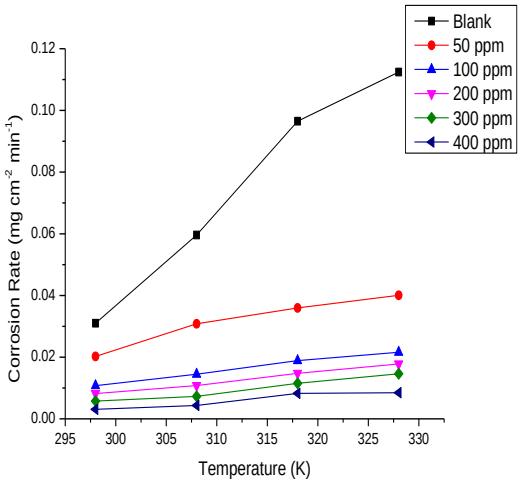

Figure 3. Relation between corrosion rate and temperature for various concentrations of the extract.

Effect of Temperature

The effect of temperature on the inhibited acid-metal reaction is very complex according to [22], because many change occur on the metal surface such as rapid etching, desorption of extract molecules and extract molecules may undergo decomposition. The influence of temperature on percentage inhibition efficiency was studied by conducting weight loss measurement at (298-328)K. At present of different concentrations of extract(Table2). The relation between the corrosion rate (k) of C-steel and temperature (T) is often expressed by the Arrhenius equation (5)[23]:

$$\log k = \log A - \frac{Ea}{2.303RT} \quad (5)$$

Where k, is the corrosion rate E^*_a, is the apparent activation energy, R, is the universal gas constant , T is the absolute temperature and A, is the frequency factor, the plot of log k against 1/T for C-steel corrosion in10%NH_2SO_3H in the absence and presence of different concentrations of extract is represent in Figure4.All parameters are given in Table3. It is clear that the addition of extract to acid solution increases the value of E^*_a. The increase in $E^*_a$is proportional to the extract concentration. Such a trend suggests that the corrosion reaction will be further pushed to the surface sites that are characterized by progressively higher values of E^*_a. as the concentration of the extract becomes larger [24]This mean that the adsorption of extract on C-steel surface lead to formation of barrier layer that retard the metal activity in the electrochemical reactions of corrosion [25]explained that the increase in E^*_a can be attributed to an appreciable decrease in the adsorption of the inhibitor on C-steel surface with in increase temperature and corresponding increase in corrosion rates due to the fact that greater area of metal is exposed to acid environment. As adsorption decrease, more desorption of inhibitor molecules occurs because these two opposite processes are in equilibrium. More desorption of extract moleculesat higher temperatures, the greater surface area of C-steel comes in contact with aggressive environment, resulting in an increase of corrosion rates with temperature. With high extract concentration, this problem is avoided because decrease of surface coverage are close to saturation [26] The increase in E^*_a after addition of extract to 10%NH_2SO_3H solution can indicate the physical adsorption (electrostatic interaction) occurs in the first stage[27] indeed extract molecule which contain heteroatom in its structure can be protonated to form cation forms in acid media . It's logical to assume that in this case the electrostatic cation adsorption is responsible for the good protective properties of this extract. However, adsorption phenomenon of an organic molecule is not considered only as physical or chemical adsorption phenomenon. [28]

Experimental corrosion rate values obtained from weight loss measurements for C-steel in10%NH_2SO_3H in the absence and presence of extract was used to further gain insight on the change of enthalpy (ΔH^*) and entropy (ΔS^*) of activation for the formation of activation complex in the transition state using transition equation(6)[29]:

$$k = \left(\frac{RT}{Nh}\right)\exp\left(\frac{\Delta S^*}{R}\right)\exp\left(\frac{-\Delta H^*}{RT}\right) \quad (6)$$

Where h is the Planck's constant N, is the Avogadro's number, ΔH^* and $\Delta S^*$are the enthalpy and entropy change of activation. Figure 5 shows the plot of log k/T versus 1/T for C-steel in10%NH_2SO_3H in the absence and presence of different concentrations of extract. Straight lines

Were obtained with slope of (ΔH^*/2.303 R) and an intercept of [log (R/Nh) + (ΔS^*/2.303 R)]

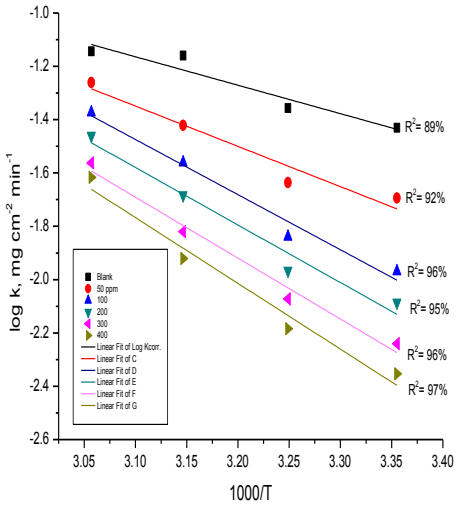

Figure 4. Arrhenius plot for C-steel corrosion in 10%NH_2SO_3H in the absence and presence of various concentration extract.

from which the value of ΔH^* and ΔS^* were computed and are listed in Table 3.

Table 2. Calculated value of corrosion rate (K) and inhibition efficiency (I%) for C-steel in 10%NH_2SO_3H in the absence and presence of extract at (298:328) K

[inhibitor]	Corrosion Rate (k) mg cm^{-2} min^{-1}				Inhibition efficiency (IE %)			
ppm	298K	308K	318K	328K	298K	308K	318K	328K
Blank	0.031	0.0596	0.0965	0.1124	--	--	--	--
50	0.0202	0.0308	0.0359	0.0400	34.7	35.0	64.0	77.9
100	0.01076	0.0145	0.0189	0.0216	65.3	67.06	80.4	83.2
200	0.0082	0.0108	0.0147	0.0178	73.5	75.5	88.0	84.2
300	0.00575	0.00731	0.01152	0.0146	81.5	83.4	88.1	87.0
400	0.0031	0.00434	0.00826	0.00848	90.0	90.2	91.4	92.5

Inspection of these data revealed that the ΔH^* values (47.7 – 67.9 kJ mol^{-1}) for dissolution reaction of C-steel in 10%NH_2SO_3H in the absence and presence of extract.

The positive sign of ΔH^* reflects the endothermic nature of C-steel dissolution process suggested that the dissolution of C-steel is slow [30]. It is also clear that $E^*_{a.}$ and ΔH^* increase with increase extract concentration. Entropy of activation, ΔS^* remains almost constant with increase of extract concentration (Table 3) and their values were negative both in the inhibited and uninhibited systems. The negative values of entropies of activation imply that the activation complex in the rate determining step represents an Association rather than a dissociation step, meaning that a decrease in disorder take place on going from reaction to the activated [31].

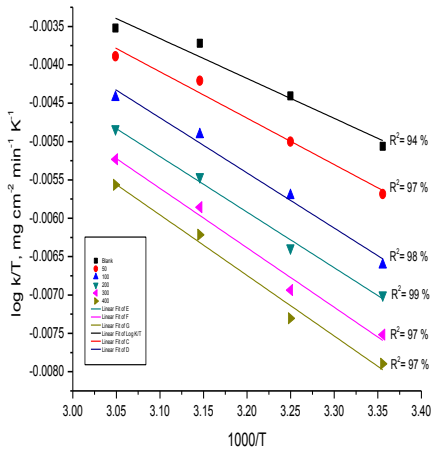

Fig 5. Transition state plot for C-steel corrosion in 10%NH_2SO_3H in the absence and presence of various concentration extract

Table 3. Activation parameters of the dissolution of C-steel in 10%NH_2SO_3H in the absence and presence of different concentration of extract.

[Inh.] ppm	$E^*_{a.}$ (kJmol^{-1})	ΔH^* (kJ mol^{-1})	$-\Delta S^*$ (J mol^{-1} K^{-1})
Blank	16.1	35.7	197.15
50	21.2	47.7	197.408
100	24.1	48.3	197.327
200	28.3	49.8	197.32
300	36.3	51.7	197.32
400	41.5	67.7	197.36

Adsorption Isotherms

It is well recognized that the first step in inhibition of metallic corrosion is the adsorption of organic molecule at the metal/solution interface. Furthermore, the adsorption depends on the molecule's chemical composition, temperature and electrochemical potential at the metal/solution interface. So the adsorption of organic inhibitor molecules from the aqueous solution can be regarded as aquasi-substitution process between organic compound in the aqueous phase [$Org_{(Sol.)}$] and water molecule at the surface of metal [$H_2O_{(ads.)}$] [32].

$$Org_{Sol.} + xH_2O_{ads.} \leftrightarrow Org_{ads.} + xH_2O_{Sol.}$$

Where x is size ratio that is the number of water molecule replaced by one organic inhibitor. Basic information on the interaction between the inhibitor of C-steel surface can be provided by the adsorption isotherms. In order to obtain the isotherm, the relation between degree of surface coverage (θ) and inhibitor concentration (C) must be found. Attempts were made to fit the θ to various isotherms including Langmuir, Temkin, Frumkin and Flory-Huggins. By far the best fit was obtained with Langmuir isotherm. This model has also been used for other inhibitor systems [33, 34]. According to this isotherm, θ is related to C by:

$$\frac{C}{\theta} = \frac{1}{K_{ads.}} + C \qquad (7)$$

Where $K_{ads.}$ Denotes the equilibrium constant for the adsorption process. Figure 6 shows the plot of C/θ versus C and the expected linear relationship is obtained with good correlation coefficients confirming the validity of the equation. The slopes were nearly unity which is an indication that Langmuir isotherm is obeyed at these temperatures (Table 4)[35].

The value of equilibrium constant of adsorption K_{ads} obtained from Langmuir adsorption isothermare listed in Table 4, together with the value of Gibbs free energy of adsorption (ΔG°) calculated from the equation (8):

$$\Delta G°_{ads.} = -RTln(55.5K_{ads}) \qquad (8)$$

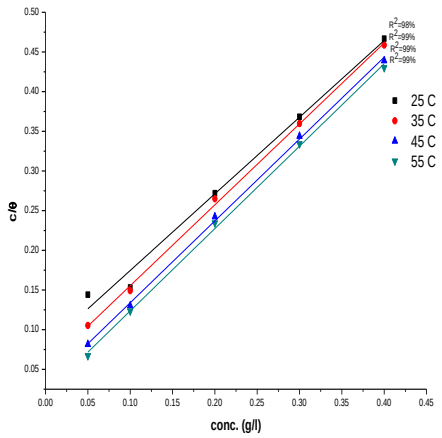

Fig 6. Langmuir adsorption plot for C-steel in the presence of extract

The value of 55.5 is the concentration of water in the solution expressed in molar. The high values of K_{ads} for

studied inhibitor indicate stronger adsorption on the C-steel surface in 10%NH_2SO_3Hsolution. This can explained by presence of heteroatom and π-electrons in the extract molecules. The stronger and more stable the adsorbed layer of the extract on the metal surface and consequently, the higher the inhibition efficiency [36].This data support the good performance of Psidium guajava leaf as green corrosion inhibitor for C-steel in 10%NH_2SO_3H solution. The negative value of $\Delta G°_{ads}$, are consistent with the spontaneity of the adsorption process and the stability of adsorbed layer on the steel surface. Generally, the values of $\Delta G°_{ads}$up to -20kJmol^{-1} are consistent with physisorption, while those around -40kJmol^{-1} or higher are associated with chemisorption as a result of sharing or transfer of electrons from organic molecule to metal surface to form coordination bond [37].In the present study, the calculated values of $\Delta G°_{ads}$ obtained in range -30.1 and -34.2 kJmol^{-1}(Table 4),indicate that the adsorption of mechanism of Psidium guajava leaf on C-steel in 10%NH_2SO_3H solutionat studied temperatures may be combination of both physisorption and chemisorption.

(Comprehensive adsorption) [38, 39] however the physisorption was the major contributor while chemisorption only slightly contributed to the adsorption mechanism.

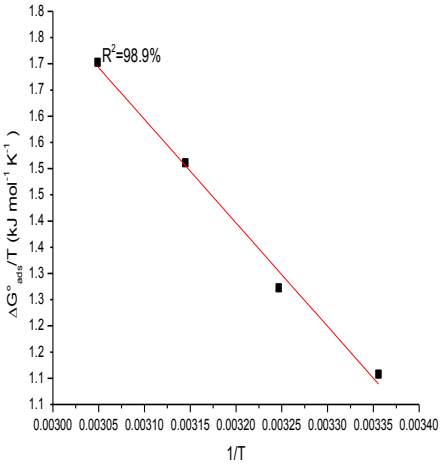

Figure 7. The variation of $\Delta G°_{ads}$ / T with 1/T.

The variation of ΔG°/T with 1/T gives straight line, the slope is equal $\Delta H°_{ads}$Fig.7 it can be seen form this Figure that ΔG°/T decreases with 1/T in linear fashion. The enthalpy and entropy for the adsorption of inhibitor on C-steel was also deduced from thermodynamic basic equation[40] (9):

$$\Delta G°_{ads} = \Delta H°_{ads} - T\Delta S°_{ads} \quad (9)$$

Entropy of adsorption obtained from equation (9) and their values were negative because inhibitor molecule freely moving in the bulk solution and were adsorbed in an orderly fashion onto C-steel, resulting in a decrease in entropy [41].

Electrochemical Methods

Open circuit potential (OCP)

Figure8 shows effect of various concentrations of Psidium guajava leaf extracton the variation OCP of C-steel with time in aerated non-stirred10%NH_2SO_3Hsolution at 298 K. The steady-state values of OCP is more negative than the immersion potential (OCP at t=0), suggesting that before the steady state condition is achieved the pre-immersion, air formed oxide film has to dissolve [42]. This steady state potential ($E_{corr.}$) which quickly achieved (after about 10 min of immersion), corresponds to the free corrosion of the bare metal[43]. It is obvious that ($E_{corr.}$) shifts to morenegative values without changing general feature of the E/t curve by increasing the concentration of extract.

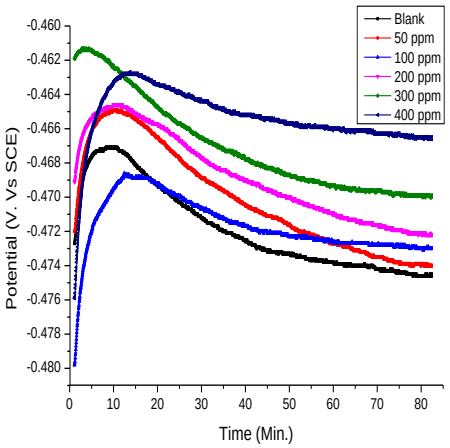

Figure 8. Variation of open circuit potential as function of time record for C-steel electrode in 10%NH_2SO_3H Solution with and without various concentrations of extract

The OCP shifted first to less negative values reaching a maximum. After certain time depending on the concentration of extract, the potential decreases and reached a reasonably steady value. These results demonstrated that two counter-acting processes occurred. The first process being the formation of a protective adsorbed layer on the electrode surface, and consequently delayed-action corrosion occurred shifting the OCP to more noble values. The second process is corrosion, which made potential back towards between these two counter-acting processes may explain the appearance of an arrest or peak in the OCP vs. time curves (Fig.8). The steady-state potential moves towards more negative values with an increase extract concentration. At first OCP shift to less negative values (due to corrosion inhibition) reaching maximum, and after certain time the potential decreased to reach a reasonably steady value (due to metal dissolution). Causes the steady state corrosion potential to move towards more negative value. These results reveal that Guava is efficiency green corrosion inhibitor.

Potentio dynamic polarization tests

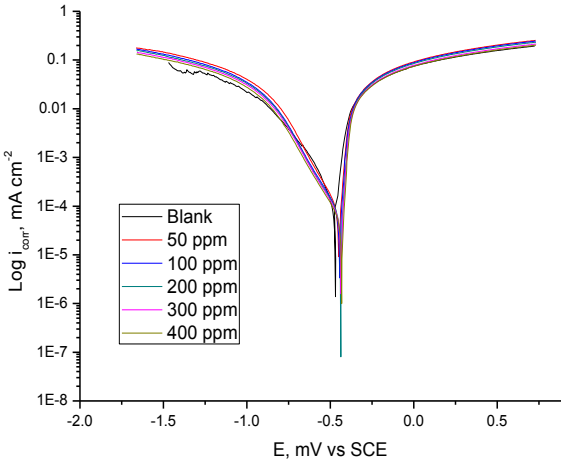

Figure 9. Potentiodynamic anodic and cathodic polarization curve of C-steel electrode in10%NH_2SO_3H solution with and without various concentrations of extract at 298K

Figure 9 shows the polarization behavior of C-steel in 10%NH_2SO_3H solution in the absence and presence of various concentration of extract.

Table 4. Showssome parametersobtained from Langmuir adsorption isotherm for C-steel in 10%NH_2SO_3H in the presence of extract

Temp. °K		Slope	$K_{ads.}$ M^{-1}	$-\Delta G°$ $kJmol^{-1}$	$\Delta H°$ $kJmol^{-1}$	$\Delta S°$ $J\ mol^{-1}K^{-1}$
298		0.965	57.82	30.1	85.8	349.50
308		1.019	90.72	31.8		346.53
318		1.031	132.45	33.6		341.24
328		1.038	1160.3	34.2		340.28

We can see clearly that both the anodic and cathodic branches of the polarization curve exhibit a typical Tafel behavior. The corrosion rate can be determined by Tafel extrapolation method [44,45].Table 5shows the electrochemical parameters (i_{corr}, E_{corr}, β_a, β_c and IE %) associated with polarization measurements of C-steel in 10% NH_2SO_3H solution in absence and presence of different concentrations of extract. Inspection of Table 5 reveals that the corrosion current (i_{corr}) decreased and inhibition efficiency increased with increased extract concentration. Also, β_a, β_c values changed slightly with the addition of the extract, indicating that this extract functions through blocking the reaction sites on the metal surface without changing the anodic and cathodic reactions mechanism. If the largest displacement of E_{corr} value surpasses ± 85 mV, the inhibitor can be cathodic or anodic type inhibitor[46]. According to the E_{corr} values listed in Table 5, the largest E_{corr} shift is 38 mV, which indicate that the extract can be classified as mixed-type inhibitor. The values (IE%) were calculated using the following equation[47]:

$$IE\% = 100 \times [(i^{\circ}_{corr} - i_{corr})/i^{\circ}_{corr}]$$

Where $i^{\circ}_{corr}$and $i_{corr}$are the corrosion current densities for uninhibited and inhibited solution, respectively. Table.5 shows that the IE% increases with increasing inhibitor concentration.

Table 5. Electrochemical parameters (i_{corr}, E_{corr}, β_a, β_c and IE%) associated with polarization measurements of C-steel in 10%NH_2SO_3H solution in absence and presence of different concentrations of extract at 298K

[inh.] ppm	$i_{corr}\mu Acm^{-2}$	$-E_{corr}$, mV vs. SEC	β_a, $mVdec^{-1}$	β_c, $mVdec^{-1}$	IE%
Blank	199.0	470	76	235	-----
50	117.0	448	67	187	41.2
100	77.7	444	45	177	61.3
200	64.0	437	34	177	67.8
300	59.3	436	36	180	72.2
400	45.2	432	30	172	77.3

Impedance (EIS) measurements

Figure 10.Represents (CPE) an equivalent circuit was proposed to corrosion of C-steel electrode in solution. Where R_s is solution resistance, $R_{ct}$is the charge transfer resistance, CPE is constant phase element is substituted for capacitive element to give more accurate fit and calculate C_{dl} the capacitance double layer [48]. This semicircle is attributed to the time constant of charge-transfer and double layer capacitance[49-51].This semicircle make an angle approaching 68.5° with real axis and its intersection gives value of 4.8 Ω cm^2 for the resistance of the solution (Rs)enclosed between the working and reference electrodes.

A good fit with this model obtained with our experimental data. It's obvious from Fig.11 that the presence and absence of Psidium guajava leaf inhibitor not change shapes of impedance plots. These results support the results of polarization measurements that inhibitor does not alter the electrochemical reactions responsible for corrosion.

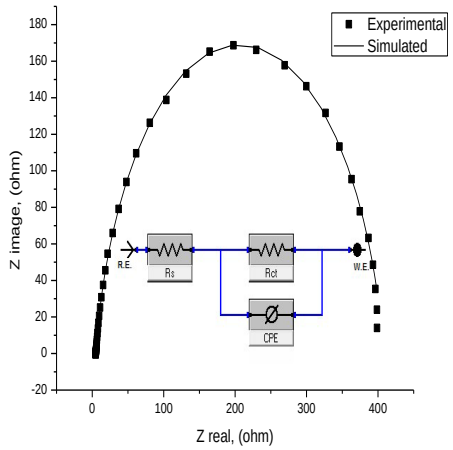

Fig 10. Complex plane impedance plot together with equivalent circuit used to fit impedance data

It inhibits corrosion primary through its adsorption on the metal surface. The point of intersection between depressed semicircle and real axis represent (R_s + R_{ct}) [43]. To obtain $C_{dl,}$ the frequency (f_{max}) at which the imaginary component of the impedance is maximal was found and then used equation (15):

$$C_{dl} = 1/2\ \pi\ f_{max} R_{ct} \qquad (15)$$

The inhibition efficiency of the inhibitor was evaluated by R_{ct}, C_{dl} and maximum phase angle (θ_{max}) should be 90° for corrosion interface represented by a simple R-C parallel equivalent circuit when Rs=0. However depressed semicircles are usually obtained for practical electrode/solution interface, which has been known to be associated with the roughness of electrode surface. Corrosion of C-steel in10%NH_2SO_3H solutions increase the roughness of the electrode surface and there for reduces the values of θ_{max}. A less depressed semicircle (with higher maximum phase angle close to 90°) also indicate better quality of inhibitor monolayer(Table6)

The values of R_{ct} and θ_{max} increase with increase in the concentration of Psidium guajava leaf, while C_{dl} values tend to decrease. It is well known that the capacitance is inversely proportional to the thickness of double layer [54]. A low capacitance may result if water molecules at the electrode interface are largely replaced by extract molecules through the adsorption [54]. The larger extract molecule also reduce the capacitance through the increase in the double layer thickness. The thickness of this protective layer increases with increase in extract concentration. This process results in a noticeable decrease in C_{dl} this trend is in accordance with Helmholtz model, given by equation (16):

$$C_{dl} = \varepsilon\varepsilon_{\circ} A/d \qquad (16)$$

Table 6. Numerical values of impedance parameter (R_s, R_{ct}, C_{dl},θ_{max} and IE%) associated with impedance measurements of C-steel electrode in 10%NH_2SO_3H solutions in the presence and absence of various concentration of inhibitor at 298K

[Inh.] ppm	Rs Ω cm^2	R_{CT} Ω cm^2	C_{dl} μF cm^{-2}	θ_{max} degree	% IE
Blank	4.632	83.2	182.0	48.2	----
50	4.027	125.3	108.4	58.9	33.6
100	4.106	205.7	83.1	61.7	59.6
200	4.286	*224.5*	82.8	63.5	63.0
300	4.574	278.3	79.7	65.4	70.1
400	4.870	402.9	66.8	68.2	79.4

Table 7. The electrochemical kinetic parameters obtained by EFM technique recorded for C-Steel electrode in 10%NH_2SO_3H solutions without and with various concentration of inhibitor at

[Inh.] ppm	i_{corr}, μA	β_a mV dec^{-1}	β_c mV dec^{-1}	CF-2	CF-3	%IE
Blank	251.80	58	225	1.9	2.9	--
50	161.70	53	147	1.9	2.9	36.1
100	94.55	52	128	1.9	2.8	62.5
200	85.34	52	122	1.9	1.3	66.1
300	67.28	52	117	1.9	1.5	73.3
400	43.75	60	99.9	1.9	3.1	82.6

Where d, is the thickness of protective layer, ξ is the dielectric constant of the medium, $\xi_\circ$ is the vacuum permittivity and A is the effective surface area of the electrode. The R_{ct} values were used to calculate the IE% values through the following equation:

$$IE\% = 100 \times \theta = 100 \times \left[\frac{R_{ct} - R^{\circ}_{ct}}{R_{ct}}\right] \quad (17)$$

Where $R_{ct}$and $R^{\circ}_{ct}$are the charge transfer resistance for inhibited and uninhibited solutions, respectively.It is apparent that the inhibition efficiency increase with increase concentration of inhibitor.

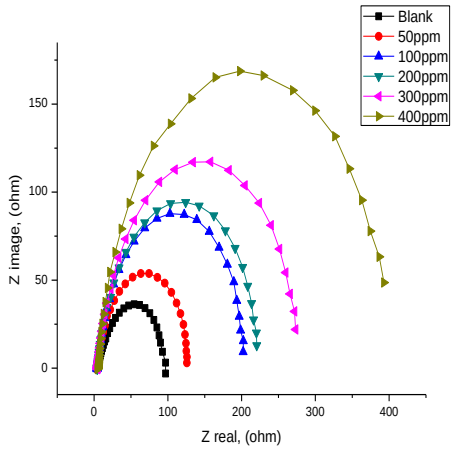

Fig 11. Complex plane impedance plots record for C-Steel electrode in 10% NH2SO3H solution in the absence and presence of various concentration of inhibitor at 298 K and at respective corrosion potential.

These results confirm the results obtained from weight loss, open circuit potential and polarization measurements, and indicate to Psidium guajava leaf inhibitor is efficacy green corrosion inhibitor.

EFM measurements

Electrochemical frequency modulation (EFM) is non-destructive corrosion measurements technique that can directly give values of the corrosion current without period knowledge of Tafel constant. Like EIS, it's a small signal ac technique unlike EIS, however two sine wave (at different frequencies)are applied to cell simultaneously. Because current is non-linear function of potential the system respond in non-linear way to potential excitation. The current response contain not onlythe input frequencies, but also contains frequency components which are the sum, difference and multiples of the two input frequencies. The two frequencies may not be chosen at random. They must both be small, integer multiples of a base frequency that determines the length of experiment. Figure 12 shows representative examples for intermodulation spectra obtain from EFM measurements. Each spectrum is a current response as a function of frequency. It is important to note that between the peaks the current response is very small. There is nearly no response (<100nA) at 4.5 Hz, for example, they are direct consequences of the EFM theory [55-56].

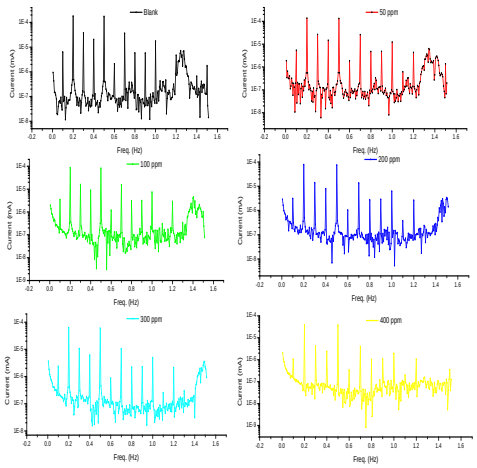

Fig 12. Intermodulation spectrum recorded for C-Steel electrode in 10% NH2SO3H solution in the absence and presence of various concentration of inhibitor at 273°K and at respective corrosion potential.

Corrosion kinetic parameter listed in Table 7are calculated from EFM technique. Table 7shows corrosion kinetic parameters such as inhibition efficiency (IE %), corrosion current density (i_{corr}), Tafel constants (β_a,β_c) and causality factors (CF-2, CF-3) as a function of inhibitor concentration in the absence and presence of inhibitor. It's obvious that $i_{corr,}$ values decrease while IE% increase with increase of extract concentration. IE% were calculated from equation (18):

$$IE\% = \theta \times 100 = (1 - \frac{i^{\circ}_{corr}}{i_{corr}}) \times 100 \qquad (18)$$

Where i°_{corr} and i_{corr} are corrosion current density in the absence and presence of inhibitor, respectively.

The great strength of EFM is causality factor which serve as an internal check on the validity of the EFM measurement [56]. With the causality factors the experimental EFM data can be verified. The standard values for CF-2 and CF-3 are 2.0 and 3.0, respectively. It is quite obvious that the data obtained from chemical and electrochemical measurement were in good agreement with the result obtained from EFM.

Scanning Electron Microscope (SEM)

Figures13-15 show SEM micrographs for C-steel surface after 24 hr. immersion in aerated 10% NH_2SO_3H solution without and with the addition of 400 ppm of Guava extract. As expected this, Fig.13in the absence of inhibitor C-steel surface is damaged by aerated 10% NH_2SO_3H solution but Fig.14in the presence of Guava extract, the metallic surface seems to be almost no affected by acid corrosion.

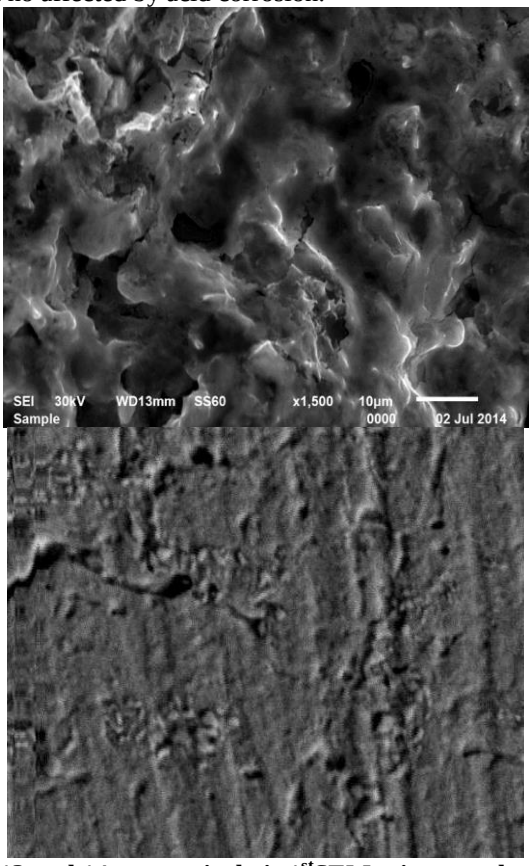

Figs 13 and 14. respectively is 1st SEM micrographs of C-steel immersed in aerated 10% NH_2SO_3H solution and 2nd is after 24hr. of immersion in in aerated 10% NH_2SO_3H + 400 ppm of Guava all at 298°K

Mechanism of Inhibition

The leaves of *P. guajava* contain an essential oil rich in cineol, tannins, triterpenes, flavanoids, resin, tannin, eugenol, mallic acid, fat, cellulose, chlorophyll, mineral salts and a number of other fixed substances [57, 58]**.**These plant products are organic in nature that are known to exhibit inhibiting action. It is therefore appropriate to say that the adsorption of these compounds onto metal surface is responsible for corrosion inhibition effect and hence difficult to assign the inhibitive effect to a particular constituent.

Conclusions

Weight loss, open circuit potential, polarization, impedance, EFM and SEM were used to study the corrosion inhibition of C-steel in 10%NH2SO3H solutions by using green corrosion inhibitor "Guava". The principle conclusions are

1-The corrosion reduce strongly with Guava and IE% increase with increase guava concentration.

2-Open circuit potential is more positive with increase Guava concentration.

3-Corrosion current decrease with increase guave concentration.

4-R_{ct}increases with increasing Guava conc. While C_{dl} decreases.

5-Physisorption is proposed as the mechanism for corrosion inhibitor.

6-The inhibition efficiencies obtained from weight loss data are comparable with those obtained from polarization, impedance and EFM measurements.

References

[1]NnabukOkon Eddy, Green chemistry letter and review (5) 2012, 43-53.

[2] K.S. Beenakumari, Green chemistry letter and review (4) 2011, 117-120.

[3] Barouni, K.; Bazzi, L.; Salghi, R.; Mihit, M.; Hammouti, B.; Albourine, A.; El Issami, S. Mater. Lett.2008, 62, 3325_337.

[4] Eddy, N.O.; Ibok, U.J.; Ebenso, E.E. J. Appl.Electrochem. 2010, 40, 445_456.

[5] Bendahou, M.A.; Benadellah, M.B.E.; Hammouti,B.B. Pigment Resin Technol. 2006, 35 (2), 95_100.

[6] Rajendran, S.; Ganga, S.V.; Arockiaselvi, J.; Amalraj,A.J. Bull. Electrochem. 2005, 2 (8), 367_377.

[7] Okafor, P.C.; Osabor, V.; Ebenso, E.E. Pigment Resin Technol. 2007, 36 (5), 299_305.

[8] Oguzie, E.E.; Onuchukwu, A.I.; Okafor, P.C.; Ebenso,E.E. Pigment Resin Technol. 2006, 35 (2), 63_70.

[9] Oguzie, E.E.; Onuoha, G.N.; Ejike, E.N. Pigment Resin Technol. 2007, 36 (1), 44_49.

[10] El-Etre, A.Y. Inhibition ofaluminium corrosion using Opuntia extract. Corrosion Sci. 2003, 45, 2485_2495.

[11] Sharma, S.K.; Mudhoo, A.; Jain, G.; Sharma, J. Rassayan J. Chem. 2009, 2(2), 332-339.

[12] A.U. Malik, I.N. Andijani, N.A. Siddiqi, S. Ahmed, A.S., Studies on the Role of Sulfamic Acid as a Descalantin Desalination Plants, Technical Report No. SWCCRDC-32 in December, Al-Jubal KSA, 1993.

[13] M. Ramananda Singh. J Mater. Environ. Sci. 4(1)(2013) 119-126

[14] A.S. Fouda, M.A. Elmorsi, T. Fayed & I.A. El said (2014): Oxazole derivatives as corrosion inhibitors for316L stainless steel in sulfamic acid solutions, Desalination and Water Treatment,

[15] N.O. Obi-Egbedi, I.B. Obot, Arabian journal of chemistry (2010): Xanthione: A new and effective corrosion inhibitor for mild steelin sulphuric acid solution

[16] Bentiss, F., Traisnel, M., Gengebre, L., Lagrenee, M., 1999. Appl. Surf. Sci. 152, 237.

[17]Sayed S. Abdel Rehim, Omar A. Hazzazi, Mohammed A. Amin, Khaled F. Khaled, corr. Sci. 50(2008)2258-2271
[18] Mohammed A. Amin, K. F. Khaled, corr. Sci. 52(2010) 1194-1204
[19] R. W. Bosch, J. Hubrecht, W.F. Bogaerts, B.C.Syrett, Corrosion 57(2001) 60
[20] S.S. Abdel-Rehim, K.F. Khaled, N.S.Abd- Elshafi, Electrochim. Acta 51 (2006) 3269
[21] B.A. Boukamp, Equivalent Circuit, Princeton Applied Research Corporation, Princeton, NJ, 1990
[22]Bentiss, F., Lebrini, M., Lagrenee, M., 2005. Corros. Sci. 47, 2915.
[23] Behpour, M., Ghoreishi, S.M., Gandomi-Niasar, A., Soltani, N.,Salavati-Niasari, M., 2009. J. Mater. Sci. 44, 2444.
[24]Mansfeld, F., 1987. Corrosion Mechanism. Marcel Dakkar, NewYork, NY, p. 119.
[25]Szauer, T., Brand, A., 1981. Electrochim. Acta 26, 245.
Umoren, S.A., Obot, I.B., Obi-Egbedi, N.O., 2009b. J. Mater. Sci. 44,274.
[26]Herrag, L., Hammouti, B., Elkadiri, S., Aouniti, A., Jama, C., Vezin,H., Bentiss, F., 2010. Corros. Sci. doi:10.1016/j.corsci.2010.05.024.
[27]Solmaz, R., Kardas, G., Culha, M., Yazici, B., Erbil, M., 2008a.Electrochim. Acta 53, 5941.
[28]Solmaz, R., Kardas, G., Yazici, B., Erbil, M., 2008b. Colloids Surf. A: Physicochem. Eng. Aspects 312, 7.
[29]Guan, N.M., Xueming, I., Fei, I., 2004. Mater. Chem. Phys. 86, 59.
[30]Obot, I.B., Obi-Egbedi, N.O., 2009. Corros. Sci. 52, 276.
[31]Sein, L.T., Wei, Y., Jansen, S.A., 2001. Comput. Theor. Polym. Sci.11, 83.
[32]Kissi, M., Bouklah, M., Hammouti, B., Benkaddour, M., 2006. Appl.Surf. Sci. 252, 4190.
[33]Machnikova, E., Whitmire, K.H., Hackerman, N., 2008. Electrochim.Acta 53, 6024.
[34]Villamil, R.F.V., Corio, P., Rubim, J.C., Agostinho, S.M.L., 1999. J.Electroanal. Chem. 472.
[35]Lagrenee, M., Mernari, B., Bouanis, M., Traisnel, M., Bentiss, F., 2002. Corros. Sci. 44, 573
[36]Bouklah, M., Hammouti, B., Lagrenee, M., Bentiss, F., 2006. Corros.Sci. 48, 2831.
[37]Li, X., Deng, S., Fu, H., 2010. Prog. Org. Coat. 67, 420.
[38] U.R. Evans, the Corrosion of Metals, Edward Arnold, London, 1960.
[39] A.M. Shams El Din, R.A. Mohammed, H.H. Haggag, Desalination 114 (1997) 85.
[40] N.P. Zhuk, Course in Corrosion and Metal Protection, Metallurgy, Moscow, 1976.
[41] A.I. Antropov, E.M. Makushin, V.P. Panasenko, Inhibitors of Metal Corrosion Tekhnika, Kiev, 1981.
[42] S.M. Reshetnikov, Inhibitors of Metal Acid Corrosion, Chimica, Leningrad, 1986.
[43] D.A. Jones, Principles and Prevention of Corrosion, MaCmillan, New York, 1992.
[44]S.K.Shukla, M.A.Quraishi, Corros.Sci. 120(2010)142
[45] S.T.Zhang, Z.H.Tao, S.G.Liao, F.J.Wu., Corros.Sci. 52(2010)3126
[46] X.Luo, S.Zhang, L.Guo, Int.J.Electrochem.Sci, 9(2014)7309
[47] B. Rosborg, J. Pan, C. Leygraf, Corros. Sci. 47 (2005) 3267.
[48] S.S. Abd El-Rehim, H.H. Hassan, M.A. Amin, Mater. Chem. Phys. 78 (2002) 337.
[49] S.S. Abd El-Rehim, H.H. Hassan, M.A. Amin, Corros. Sci. 46 (2004) 5–25.
[50] Mohammed A. Amin, J. Appl. Electrochem. 36 (2006) 215.
[51] X. Wu, H. Ma, S. Chen, Z. Xu, A. Sui, J. Electrochem. Soc. 146 (1999) 1847.
[52] S.S. Abdel Rehim, H.H. Hassan, M.A.Amin, Appl. Surf. Sci. 187 (2002) 279.
[53] O.E. Barcia, O.R. Mattos, N. Pebere, B. Tribollet, J. Electrochem. Soc. 140 (1993)
2825.
[54] C. Deslouis, B. Tribollet, G. Mengoli, M.M. Musiani, J. Appl. Electrochem. 18 (1988) 374.
[55] (a) B.A. Boukamamp, Solid State Ionics 20 (1980) 31;
(b) International Report CT 89/214/128, University of Twente, Eindhoven, The Netherlands (1989).
[56] A. V Benedetti, P.T.A. Sumodjo, K. Nobe, P.L. Cabot, W.G. Proud, Electrochim. Acta 40 (1995) 2657.
[57] H.M.Burkill, The Useful Plants of West Tropical Africa. Royal Botanical Gardens, Kew2Ed., London, 1997
[58] O.A. S.O. Olajide Awe and J.M. Makinde, Pharmacological studies on the leaf of *Psidium guajava*. Fitoterapia, 70(1999).: 25-31.